

Fe Analysis of Residual Stresses Induced by Spot Welding of Stainless Steel Type AISI 316

Dr. Ahmed N. Al-Khazraji

Mechanical Engineering Department, University of Technology / Baghdad

Dr. Samir A. Al-Rabii

Mechanical Engineering Department, University of Technology / Baghdad

Email:alrabiee2002@yahoo.com

Ali Hussein F. Al-Jelehawy

Mechanical Engineering Department, University of Technology / Baghdad

Revised on: 6/2/2013 & accepted on: 5/9/2013

ABSTRACT

Specimens of the as-received stainless steel type 316, according to AISI standard, in form of sheet with 1.5 mm thickness were first spot welded and then shot peened to obtain the influence of shot peening process on the residual stresses induced by spot welding process. X-Ray Diffraction (XRD) method was used to measure the residual stresses. Also, a finite element method (FEM) was employed by ANSYS software version 11 to achieve the simulations for transient thermal analysis and residual stresses analysis in all cases. In addition, the temperature dependency of materials properties was used to assess its effects on the final residual stress results. A comparison showed a very good agreement between the experimental and the numerical results due to the total elimination of tensile residual stresses and creating the compressive type instead.

Keywords: Stainless Steel, Residual Stresses, XRD, Stress Relief, Shot Peening, FEM.

التحليل بالعناصر المحددة للأجهادات المتبقية المتولدة من عملية اللحام النقطة
للصلب المقاوم للصدأ نوع AISI316

الخلاصة

تم إجراء عملية اللحام النقطة لعينات في الحالة المستلمة للصلب المقاوم للصدأ نوع (316) وفقاً للمواصفة (AISI) بشكل صفائح وبسمك (1.5) ملم وتم بعد ذلك سفعها بالكريات لبيان تأثير عملية السفع على الأجهادات المتبقية المتولدة من عملية اللحام النقطة. استخدمت طريقة حيود الأشعة السينية (XRD) لقياس الأجهادات المتبقية. تم تطبيق طريقة العناصر المحددة (FEM) أيضاً باستخدام برنامج (ANSYS 11) لإنجاز المحاكاة لكل من التحليل الحراري الانتقالي وتحليل الأجهادات المتبقية في جميع الحالات. إضافة إلى ذلك، استخدم تأثير درجة الحرارة على خواص المواد لتقييم تأثيرها على النتائج النهائية للأجهادات المتبقية. وظهرت المقارنة وجود توافق تام بين النتائج العملية والنظرية بسبب التخلص التام من الأجهادات المتبقية الشديدة وتوليد أجهادات ضغطية بدلاً منها.

INTRODUCTION

Welding is a complicated process accompanied by shrinkage effects, phase transformation and arising of residual stresses. Residual stresses remain in a body if all external forces or thermal gradient after yield point were removed [1]. These stresses can be quite large, and the tensile residual stresses have a dangerous effect on the engineering properties. Heat from welding causes a localized expansion which is taken up during welding by either the molten metal or the placement of parts being welded. The tensile residual stresses are not preferred in any specimen because of its effective in fatigue life under dynamic loading, crack initiation and propagation and corrosion, which lead to failure [1].

After welding, a non-uniform temperature distribution for the welded zone introduces the tensile residual stresses, it can have a dangerous effect on the material by reducing the fatigue life of metal, crack propagation, brittle fracture and stress corrosion [2]. The spot welding process consists of four stages: squeeze cycle, weld cycle, hold cycle and off cycle [3].

Some researchers investigated the effect of resistance spot welding variables, such as weld current, weld time, electrode force and surface condition of the parts to be welded on the strength of spot welds of different materials, such as wrought heat-treatable aluminum stresses alloys, austenitic stainless steel (321) [4], steel and nickel base alloys [5] using the X-ray diffraction method to measure the residual stresses. While, other previous works focused on the development [6,7], modeling and simulation [8], simulation [9,10], model prediction [11], numerical study [12], fatigue strength assessment [13], distribution of the residual stress [14], and structural integrity assessment [15]. Since there is a little work devoted to the simulation of the spot welding process using the FEM, especially stainless steel type 316 with a suitable analysis.

Therefore, the aim of this paper is first to remove the tensile residual stresses induced from spot welding 316 stainless steel sheets using shot peening process, the X-RAY diffraction method will be used to measure the residual stresses created by the spot welding process. Also, this research is then devoted to verify the experimental results by finite element method (FEM) using ANSYS software version 11 to simulate the nonlinear transient thermal analysis and nonlinear residual stresses analysis for spot welded specimens, the influence of both temperature dependency of material properties and heat generation value will be determined in addition to the comparison between the experimental residual stresses measured by the X-ray diffraction method with the numerical results obtained by the ANSYS analyses.

EXPERIMENTAL WORK

The as-received (rolled and annealed) stainless steel type AISI 316, in form of sheet with 1.5 mm thickness was first cut to prepare specimen with a dimension of (1.5 mm x 55 mm x 55 mm) for chemical composition, mechanical properties and X-ray diffraction tests. The result of chemical composition of the used material is given in Table (1) together with the standard stainless steel type 316 for comparison purpose. Also, the tensile tests were conducted for this material to obtain the mechanical properties, and the results are listed in Table (2). Also, Table (3) lists the welding parameters, and the shape of electrode used is tapered

cylindrical end. The specimens were then classified into four groups according to type of process, as listed in Table (4).

X-ray diffraction (XRD) tests were carried out for the as-received specimens in order to measure the residual stresses caused by the previous history of the mechanical working (rolling process) performed during the manufacturing of the sheet metal. These tests indicated that the residual stresses in these specimens are essentially tensile type and have lower magnitude, as shown in Table (4). All X-Ray diffraction tests were performed in the Ministry of Science and Technology by a machine shown in Figure (1). With a supplied voltage of (40KV) and current (20MA). The target is copper with a wave length ($\lambda=1.5406 \text{ \AA}$) and the filter is nickel.

Stress relief process was selected as a proper heat treatment to eliminate or reduce the tensile residual stresses of the specimens in the as-received condition. The specimens were heated in an electrical furnace, and the maximum temperature for this furnace is (1100°C). The stress relieving treatment that applied to impart the greatest degree of stress relief and to reduce the residual stress. Stress relieving was employed at a temperature of (400°C) according to ASTM, for light section, held at this temperature for 60 minutes, and then these plates were rapidly cooled by air. The measurements of the XRD tests of the stress relieved specimens showed that these tensile residual stresses are greatly reduced to a minimum level, see Table (4).

The stress relieved specimens were then spot welded at a welding time of (0.2 sec) for the sake of obtaining the influence of these duration times on the induced residual stresses by this process. This welding time was selected according to material thickness and type. After spot welding, these specimens were tested by XRD machine to measure the created residual stresses. These residual stresses were found high with a tensile type see Table(4). (80-100) % coverage and spot diameter of (2 mm). Figure (2) shows the plate after heat treatment, spot welding and shot peening.

THEORY AND FINITE ELEMENT MODELING PROCEDURE

Spot welding is a process joining technology using electrical resistance heat of metallic, and it is a complicated phenomena. The FEM analysis was carried out in two steps (coupled-field analysis that couples between two or more fields of engineering). A non-linear transient thermal analysis was first conducted to obtain the global temperature history generated during the welding process. A stress analysis was then developed with the nodal temperatures obtained from the thermal analysis, which are applied as “body force” in the subsequent stress analysis. Then, by using the result from the stress analysis with pre-stress on a static and dynamic structural analysis was achieved [16]. ANSYS (11) software was used with a 3-D model, solid 20-node element for a half upper plate, as shown in Figure (3).

The accuracy of the FEM depends on the density of the mesh used in the analysis; both stress and thermal analysis have identical mesh. The weld nugget temperature is higher than the melting point of the material, and it drops sharply in regions away from the weld nugget. Therefore, in order to obtain the correct temperature field in the region of high temperature gradients, it was necessary to have a more refined mesh closed to the weld nugget. While in regions located away from the weld-nugget, a more coarse mesh was used. Sensitivity analysis of mesh

density was performed and a satisfactory mesh was adopted for further studies, the higher is the heat input the higher is the number of nodes necessary to accurately interpolated high temperature gradient [6].

Non – Linear Transient Heat Transfer Numerical Model

One of the fundamental problems in the analysis of heat flow during welding is how to take into account the physical material changes due to temperature changes during the welding and cooling process. If the material properties are treated as temperature dependent, then the following equation of heat –flow becomes non-linear [17].

$$r \frac{\partial c_p T}{\partial t} = Q + \frac{\partial (k_x \frac{\partial T}{\partial X})}{\partial X} + \frac{\partial (k_y \frac{\partial T}{\partial y})}{\partial y} + \frac{\partial (k_z \frac{\partial T}{\partial Z})}{\partial Z} \dots\dots(1)$$

Where, c_p is the specific heat, k is thermal conductivity, T temperature, Q is the volumetric heat generation and t is time .If the material properties are considered temperature independent, this equation (specific heat, thermal conductivity do not change with temperature) is reduce to a linear partial differential equation.

$$r c_p \frac{\partial T}{\partial t} = Q + K (\frac{\partial (\frac{\partial T}{\partial X})}{\partial X} + \frac{\partial (\frac{\partial T}{\partial y})}{\partial y} + \frac{\partial (\frac{\partial T}{\partial Z})}{\partial Z}) \dots\dots(2)$$

In the present analysis, temperature-dependent material thermal properties were assumed; therefore, non-linear equations were obtained and solved. To determine temperature and other thermal quantities that vary over time, there was a need to perform a transient thermal analysis. Implicit method of time discrimination was employed which allows for larger time steps. It is important not to forget that time step size is not a problem with respect to calculation stability, but it determines the accuracy of the solution.

Using the FE analysis, the thermal and stress analysis are uncoupled, while in reality the thermal effect and mechanical deformation occur at the same time. The de-coupling of the analysis becomes acceptable if one assumes that the dimensional change (mechanical deformation) during welding process are negligible, because the thermal energy change is predominant over mechanical work done during welding, and the internal energy dissipation effect on the temperature distribution is negligible. Therefore, to evaluate distortion and residual stress distribution, the thermal analysis was first performed in order to find nodal temperature as a function of time. Once defining temperature history for each node, temperature loads were applied to the structural model. Resistance to the high electric current passing through the joint generates the heat within a spot weld totally and consequently the points of greatest heat generation are the points of greatest resistance (faying surface), were the resistance of the joint to be 80% at the faying surface and 10% at each electrode [20]. The plate absorbs a part of the heat generated. There are losses from the surfaces in the form of convection. Therefore, to evaluate the amount of heat absorbed by the plates as a portion of the total heat generated, the following formula was used [19],

$$Q = I^2 R t \quad \dots (3)$$

Where I is the welding current, R is the faying surface resistance and t the time of welding.

The assumptions made are:

- Thermal properties, i.e., conductivity, specific heat and convection are temperature dependent.
- Effects arising from phase change are taken into account.
- Heat losses by transfer to the ambient medium by radiation are taken into account.

The convective heat losses from the exterior surface can be found by Newton's law of cooling [20],

$$Q_i = hA_i(T_i - T_0) \quad \dots (4)$$

Where h is the convection heat transfer coefficient (for free convection in air, h has maximum value of $(9W/m^2 - ^\circ C)$, [73]. Q_i denotes the heat loss on surface i with area A_i , T_i is the temperature on surface A_i and T_0 is the ambient temperature.

During the welding process phase change occurred, to account the effect of latent heat, i.e., heat energy which is released or stored by the material during a phase change enthalpy was specified. The concept that could be readily adopted by the finite element was formulated on the basic of integrating the heat capacity of the material over a small region of phase changes, [21]. Thus,

$$H(T) = \int r C_p(T) dT \quad \dots (5)$$

ANSYS (11) provides many various elements to be used to analyze different problems. Selecting the correct element type is very important part of the analysis process, for this analysis (SOLID 90) was chosen. The element has 20 nodes with a single degree of freedom, temperature, at each node. The elements have compatible temperature shapes and are well suited to model curved boundaries; it was applicable to a 3-D, steady-state or transient thermal analysis. The geometry, node locations, and the coordinate system for this element are shown in Figure (4). A prism, tetrahedral, and pyramid-shaped element may be formed.

Non-Linear Numerical Model for Residual Stress

An important problem in the analysis of residual stresses during welding is how stress develops in region near the welding nugget when structural members are joined by spot welding. The material of the plates has to be heated to its melting point and then cooled again rapidly under restraint conditions imposed by the geometry of the joint. As a result of this severe thermal cycle, the original microstructure and properties of the metal in a region close to the weld are changed. This part of the metal, or zone, is usually referred to as heat-affected zone (HAZ). The change in HAZ is dependent upon the thermal and mechanical history of the metal. Therefore, after the welding process, there will be different zones with different mechanical properties. In particular, there is a softening of the material in the HAZ, and decrease of mechanical properties. After calculating the temperature

distribution with time, the next step was to find the distortion and residual stress distribution.

RESULTS AND DISCUSSION

Referring to Tables (1 and 2), the results show that the both the chemical composition and mechanical properties of the used 316 stainless steel sheet material in the as-received condition conform with those for the standard one. From the X-ray tests, the data of the diffraction angel (θ), at a tilting angle ($\psi = 50^\circ$), was obtained and then used to find the lattice spacing from Bragg's law, the residual strain and the residual stress. Table (4) depicts the results of the calculated residual strains and residual stresses, depending on the obtained by the X-ray tests. From this table, it is noticed that the X-ray diffraction data shows that the plates, in the as received condition, have tensile residual stresses but not much higher because of effect of previous the mechanical operations, like cutting, grinding, rolling. Also, the stress relief is one of heat treatment types that help to eliminate or decrease the tensile residual stresses aiming to reach the zero level. Generally, welding causes the highest tensile residual stresses and shot peening results in compressive residual stresses, as seen from previous table. It is found that this spot welding has the proper welding parameters for the residual stresses, since it has a tensile residual stress after spot welding and a compressive residual stress after the shot peening process.

Nonlinear Transient Thermal Analysis

The specimen employed was made of austenitic stainless steel type (316), sheets with nominal thickness of (1.5 mm) as described in the experimental chapter. The nonlinear transient heat transfer FE analysis requires multiple sub steps within each load step to cover the welding process time and the cooling down time until the plate reached the ambient temperature. The elapsed analysis time was 750 sec, [(0.2 sec) time for spot welding process] and the other time for cooling process. With the first load step, from 0 to 0.2 sec, smaller time step of 0.005 sec was adopted during the welding process in order to capture the melting point. Larger time step was adopted during the cooling down process.

The temperature history for the center point of spot nugget of (1.5 mm) plate thickness is presented in Figure (5 and 6), showing temperature distribution at a path along the plate through the spot with different elapsed times, during and after welding. The nodal thermal distributions with different time steps are shown in the Figures (7, 8and9). It was seen that the maximum temperature reached (1492°C) in the center of the spot or nugget zone (NZ) and then decreased and distributed along the plate. This thermal information predicted from the FE analysis was subsequently used to calculate the residual stress at various locations throughout the weldment.

Nonlinear Residual Stress Analysis

Welding processes are the most significant causes of residual stresses. When structural plates are joined by spot welding, the temperature increases rapidly to the melting point at the nugget area and reaches high temperature values at the surrounding joint. After welding, the plates are cooled rapidly and consequently gain their original yield strength. During this process of increasing and decreasing the temperature, residual stresses are developed.

Figure (10) shows the stress history at the center point of spot in the X direction. It can be seen that the initial expansion of material due to the temperature increases and constrained by material placed away from the heat source, the compressive stresses were generated first. During the cooling phase after a time of 0.2 s the temperature decreases and the stress in the solidifying material increases and becomes tensile due to the positive temperature gradient. Then at a time of 10 sec the stress reached high tensile value at the center of nugget spot, after a time it is cooled and the stress reached the steady state. Typical curves of residual stress at faying surface of the weld versus temperature at the center are shown in Figure (11). According to this figure, it is obvious that when the spot welding process begins, the compressive residual stresses will induce during that time (0,20 sec), at which the temperature increases, reaching to their maximum value of (-140 MPa) at about (700°C). Then, these stresses begin to decrease gradually till reaching the melting temperature (1492°C). After releasing the welding electrodes from the welded part, the compressive residual stresses start to transform to tensile stresses during cooling the part in air until the value of tensile residual stresses reaches the maximum which is (333 MPa).

Figure (12) shows the stress history of a point of 5mm away from the nugget center, it is clear from this figure that the stress increased rapidly in negative sign (compression) and then decreased after a time, but still in compression when it is cooled.

The stress distributions at a path of plate from the bottom center of the spot to the left edge at different times during and after welding are shown in Figure (13).

From this figure, it is clear that the longitudinal residual stresses are compression at the beginning of welding until the temperature reached the maximum value at a time of 0.2 sec and then after cooling, the longitudinal residual stress turns to tensile at the spot center area and then decreases and changed to compression residual stress away from the nugget spot, this distribution of residual stress is similar in qualitative manner to the residual stresses obtained by Dong, et al. [22], for aluminum, although the residual stress magnitude for stainless steel is higher due to its high yield strength.

The Von Mises, X - Z, and Y stress distributions are shown in the Figures (14-16) and the numerical results of the residual stresses determined by the ANSYS are given in Table (5). The maximum tensile stress is 312 MPa (X-Z direction stress), exceeding the yield stress of parent plate material. This peak tension of (312 MPa) is at the spot center or nugget zone (NZ). A comparison between the experimental result (300.4 MPa) measured by the XRD test and the numerical result obtained by ANSYS analysis for the tensile residual stresses is given in Table (6), indicating a very good agreement between the experimental and numerical results.

Figure (17) shows the finite element nodal solution, Von Mises plastic strain distribution after the weld cools to the room temperature. The maximum plastic strains concentrated at the center nugget and then gradually disappear away from the spot area. The Von Mises plastic strain vs. time at the center nugget can be seen in the Figure (18). It clears that the plastic strain increased rapidly during welding time and then still constant after welding until reached the room temperature.

Effect of Temperature Dependency of Material Properties

In real life, temperature-dependent material properties are not easily obtained, so that the average values of thermal properties over the applied temperature distribution were used to study the effect of temperature dependent material properties on the final residual stress results. Also, the yield stress at various temperatures was studied. Figure (19) shows the significant difference finite elements residual stresses obtained from the model using constant thermal properties and that using temperature-dependent material properties, especially away from the nugget spot due to the fact that the yield strength variation at higher temperature has less effect. This clearly shows the importance of the temperature dependence of material properties on the residual stresses results.

CONCLUSIONS

1. Tensile residual stresses induced by spot welding process achieved in this work are dangerous, and this result is an agreement with the other previous works.
2. Stress relief process by heat treatments and shot peening employed in this research exhibited positive results by transforming the tensile residual stresses to compressive stresses.
3. The maximum temperature reached was found to be (1492°C) in the center of the spot or nugget zone (NZ) and then decreased and distributed along the plate.
4. The compressive residual stresses induced during the spot welding process, they changed to the tensile residual stresses during the cooling.
5. It was found that the maximum tensile residual stress measured by the XRD method is 300MPa, while the maximum numerical tensile residual stress numerically determined by the ANSYS analysis is 312 MPa (X-Z direction stress) at the spot center or nugget zone (NZ), indicating a very good agreement between the experimental and numerical results.
6. It was shown that there is a very good agreement between the experimental residual stresses measured by the X-ray diffraction method and the numerical result analysis by ANSYS.

REFERENCES

- [1]. Vladimir I. Monin, Tatiana Gurova, X. Castello and S .F .Esteven, “Analysis of Residual Stress State in Welded Steel Plates by X-Ray Diffraction Method”, Advanced Study Center Co. Ltd., 2009.
- [2]. S. E. Mirsalehi and A. H. Kokabi, “ Fatigue life estimation of spot welds using a crack propagation-based method with consideration of residual stresses effect”, Materials Science and Engineering, No. A 527, pp.6359–6363, June, 2010.
- [3]. Bin Niu, Yonglin Chi and Hui Zhang, “Dynamic Electrode Force Control of Resistance Spot Welding Robot”, IEEE (International Conference on Robotics and Biomimetics), 2012.
- [4]. Ahmed M. Abdul-A’ima, “Spot Welding Efficiency and its Effect on Structural Strength of Gas Generate and Its Performance”, M.Sc. Thesis, Mechanical Engineering Department, University of Baghdad, June, 2002.
- [5]. Paul S. Prev y, “ X-Ray Diffraction Characterization of Residual Stresses Produced by Shot Peening”, Lambda Technologies, Shot Peening Theory and

- Application, series ed. A. Niku-Lari, IITT-International, Gournay-Sur-Marne, France, pp. 81-93, 1990.
- [6]. Huh, H. and W. J. Kang, "Electrothermal Analysis of Electric Resistance Spot Welding Processes by a 3-D Finite Element Method", *Journal of Materials Processing Technology*, 63, pp. 672-677, 1997.
- [7]. Feng, Z. S. S. Babu, M. L. Santalla, B. W. Rimer, and J. E. Gould, "An Incrementally Coupled Electrical- Thermal-Mechanical Model for R.S.W." 5th International Conference on Trends in Welding Research, Pine Mountain, GA, U.S.A., pp. 1-5, 1998.
- [8]. Aravinthen, A. "Modeling and Simulation of Spot Welding Process, An overview" Ph.D. Thesis, Nottingham Trent University, 2000.
- [9]. Srikunwong, C. T. Dupuy, and Y. Bienvenu, "Numerical Simulation of Resistance Spot Welding Process Using FEA Technique", ARCELOR Group, Dunkirk, France, 2002.
- [10]. Sun, X. and P. Dong, "Analysis of Aluminum Resistance Spot Welding Processes Using Coupled Finite Element Procedures", *Welding Research Supplement*, pp. 215-221, August, 2000.
- [11]. Xin Long, "Finite Element Analysis of Residual Stress Generation During Spot Welding and its Affect on Fatigue Behavior of Welded Joint", Ph.D. Thesis, University of Missouri-Columbia, December, 2005.
- [12]. Chang, B. H. and Y. Zhou, "Numerical Study on the Effect of Electrode Force in Small-Scale Resistance Spot Welding", *Journal of Materials Processing Technology*, Vol. 139, pp. 635-641, 2003.
- [13]. Bae, D. H. I. S. Sohn, and J. K. Hong, "Assessing the Effects of Residual Stresses on the Fatigue Strength of Spot Welds", *Welding Journal*, pp. 18-23, January, 2003.
- [14]. YAJIANG, LI. WANG JUAN, CHEN MAOAI and SHEN XIAOQIN, "Finite element analysis of residual stress in the welded zone of a high strength steel", *Indian Academy of Sciences*, No. 2, Vol. 27, pp. 127-132, April 2004.
- [15]. ViorelDeaconu, "Finite Element Modeling of Residual Stress - A Powerful Tool in the Aid of Structural Integrity Assessment of Welded Structures", 5th Int. Conference Structural Integrity of Welded Structures (ISCS2007), Timisoara, Romania, - Testing & risk assessment in the development of advanced materials and joints, pp. 20-21, Nov, 2007.
- [16]. Meo M, Vignjevic R. *Welding Simulation Using FEM*. World Conference, Malaysia., July 1999.
- [17]. Cosmos/ M. Finite Element Software, *Advanced Modules Theoretical Manual* SRAC, Los Angeles, California, USA, 2000.
- [18]. Lindh and J. L. Tocher, D. V. "Heat Generation and Residual Stress Development in Resistance Spot Welding", *Welding Journal*, Vol.46, No.8, pp. 331-358, 1967.
- [19]. Milner and R. L. Apps, D. R. "Introduction to Welding and Brazing", *Library of Congress Catalog*, 1968.
- [20]. Chapman, A. J., "Fundamentals of Heat Transfer", Macmillan, New York. 1987.
- [21]. Tekriwal P., Mazumunder J., "Finite Element Analysis of Three Dimensional Transient Heat Transfer in GMA", *Welding Journal*, 1988.

[22]. Wu, A. S. Syngellakis and B. G. Mellor, “Finite Element Analysis of Residual Stresses in a Butt Weld” Material Research Group, University of Southampton, Highfield, Southampton, SO17 IBJ, 2001.

Table (1) Chemical composition (wt %) of the measured 316 stainless steel

Elements		C%	Mn%	Cr%	Ni%	Mo%	Fe%
Standard AISI 316	Min			16.00	10.00	1.00	Balance
	Max	0.08	2.00	18.00	14.00	2.00	
Measured		0.08	1.05	16.39	12.21	1.15	Balance

Table (2) Mechanical properties of the used 316 stainless steel.

Alloy	σ_y (MPa)	σ_u (MPa)	EL%
Standard ASIS 316	≥ 205	≥ 515	≥ 40
Measured	298	520	40

Table (3) Spot welding parameters.

Current	Weld Time	Hold Time	Electrode Diameter	pressure
10.450 KA	0.2 sec	0.06 sec	6mm	4.4 bar

Table (4) Groups of measured residual stresses and strains .

Residual stress (MPa)	Residual strain	Type of process	Group
49	1.86801×10^{-4}	As received	A
6.5	2.490691×10^{-5}	Stress relief	B
300	11.45717×10^{-4}	Spot with 10 cycle (0.2 sec)	C
- 333	-12.70252×10^{-4}	After shot peening	D

Table (5) Maximum tensile residual stresses for all spots (numerically).

Residual stresses (MPa)		
Experimental	Numerical	Error%
300	312	3.86%

Table (6): Comparison between the experimental and numerical analysis for the tensile residual stresses

Y-Direction Stress (MPa)	Von Mises residual stresses (MPa)	Longitudinal residual stresses (MPa)
40	276	312



Figure (1): X-Ray Diffraction Machine.



Figure (2): Plate after heat treatment, spot welding and shot peening.

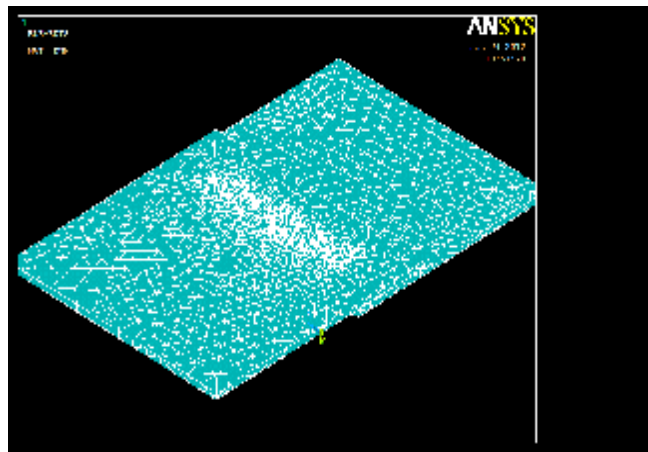


Figure (3): Finite Element Model and Mesh.

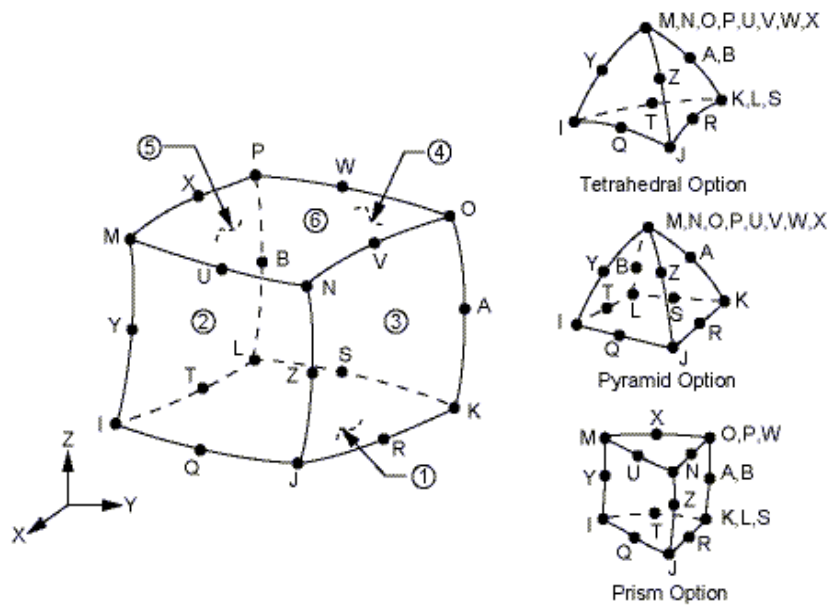


Figure (4): SOLID 90, 95 Geometry

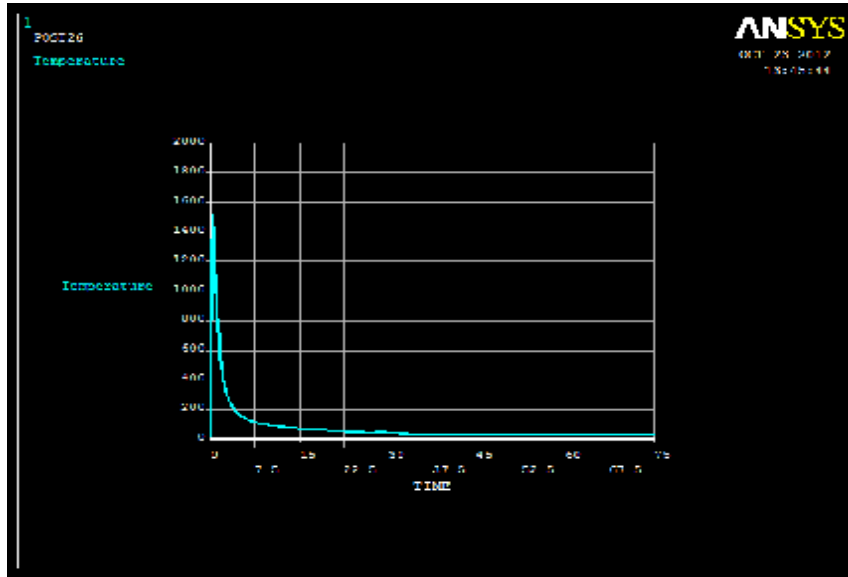


Figure (5): Temperature History at Spot Center.

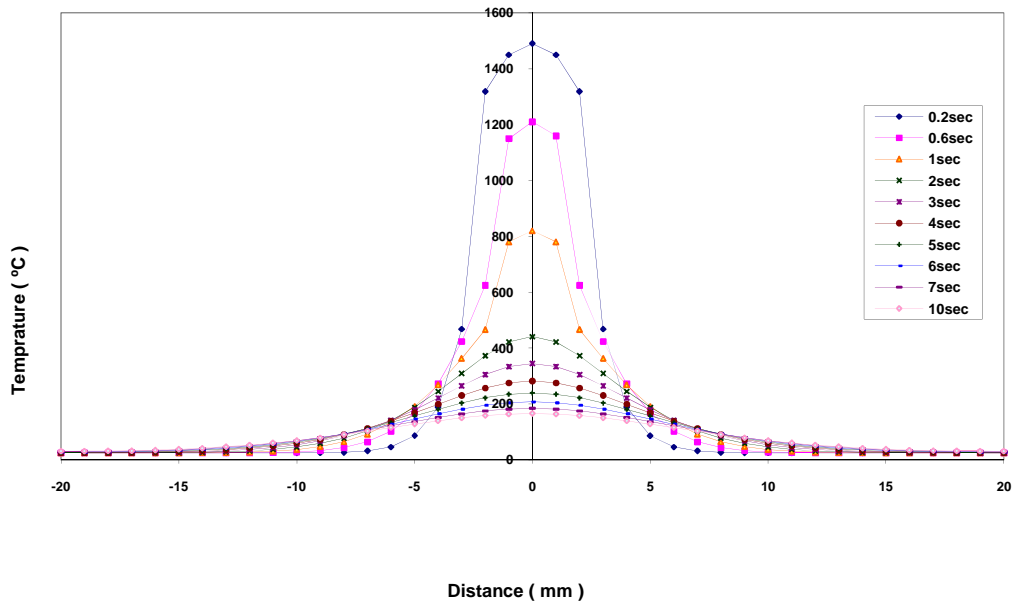


Figure (6): Temperature Distribution in X Direction 1.5 mm Plate

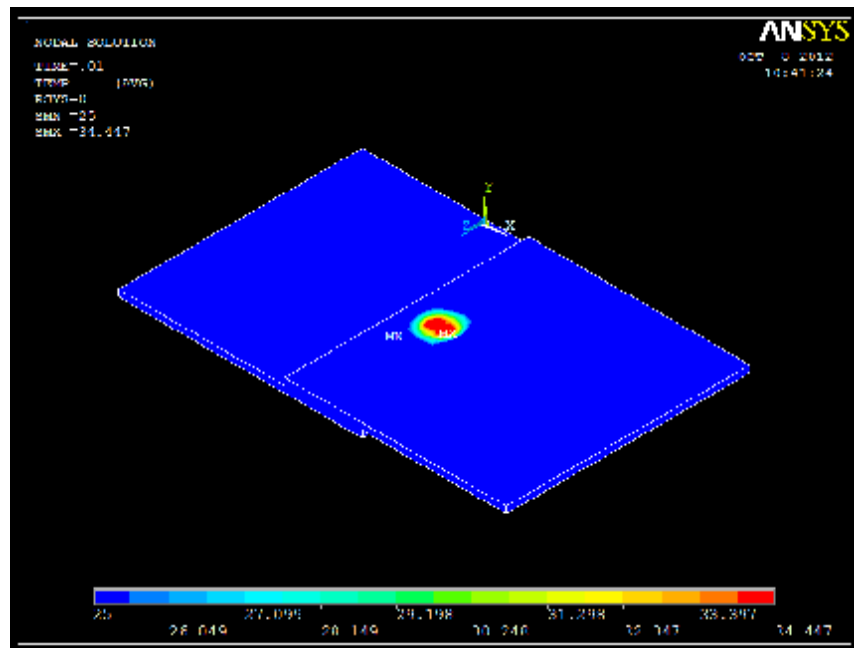


Figure (7): Temperature distribution at elapsed time = 0.01 sec.

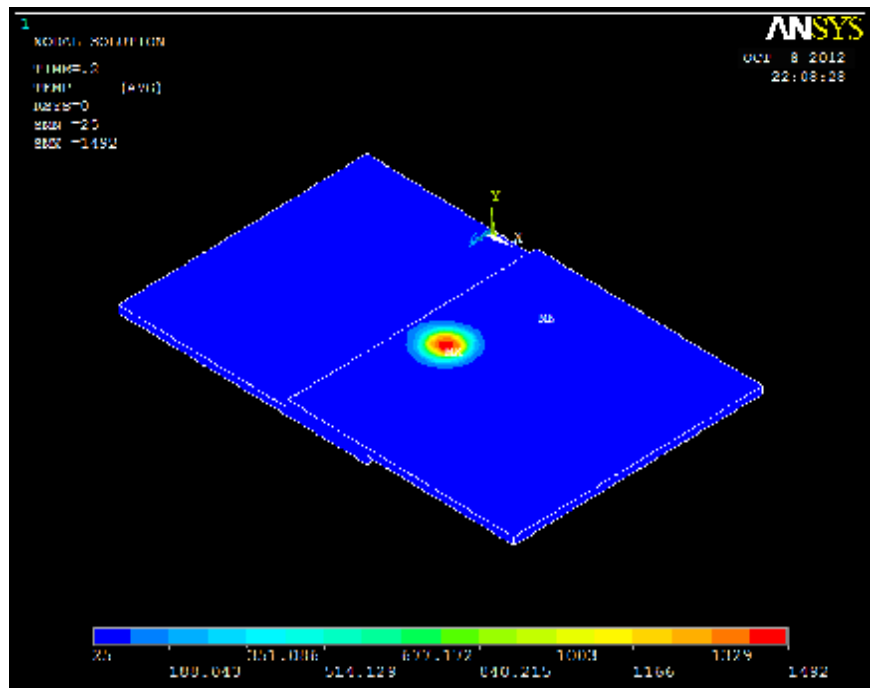


Figure (8): Temperature distribution at elapsed time = 0.20 sec.

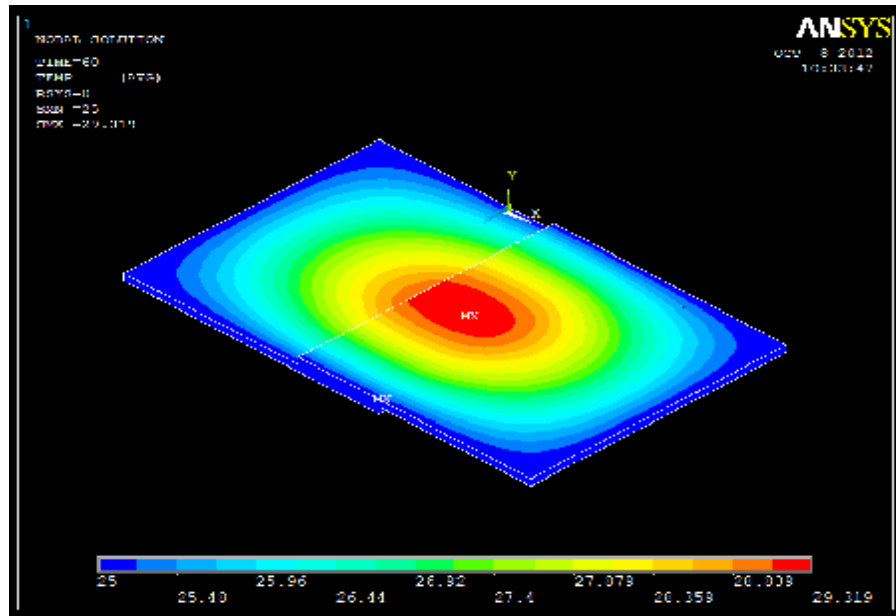


Figure (9): Temperature distribution at elapsed time = 60 sec.

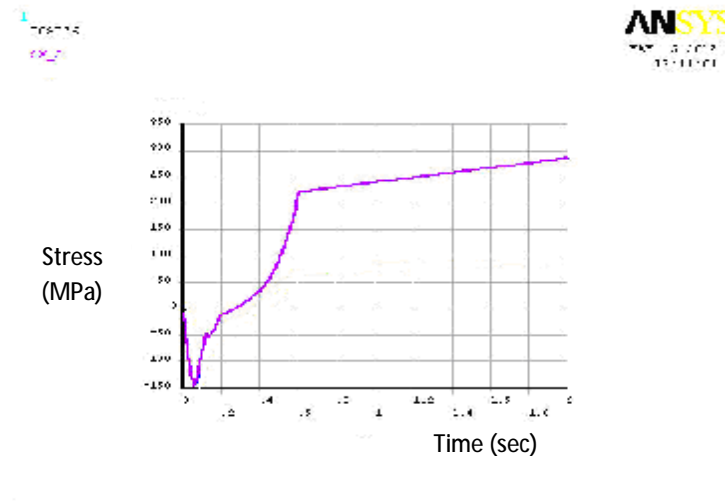


Figure (10): Longitudinal Stress History at spot Center.

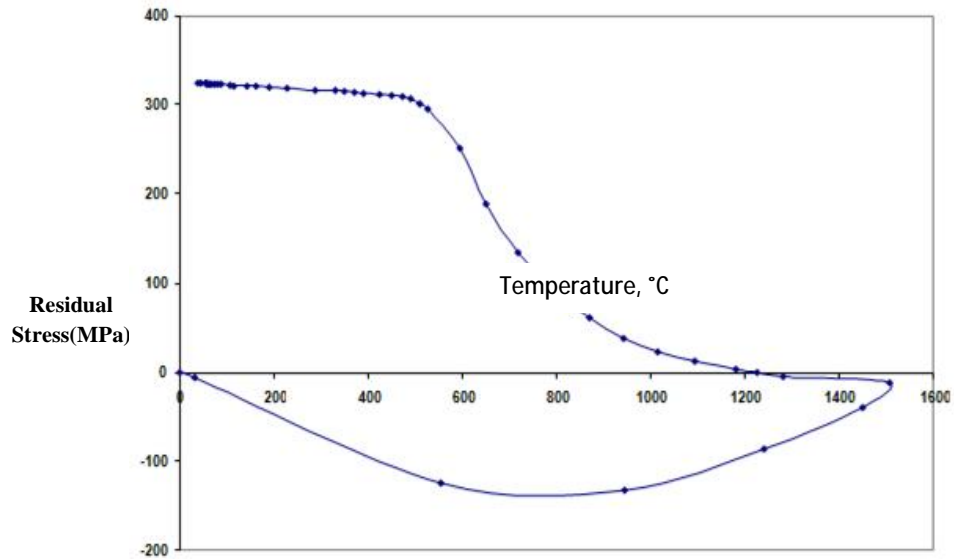


Figure (11): Stress Path during Welding at Spot Center.

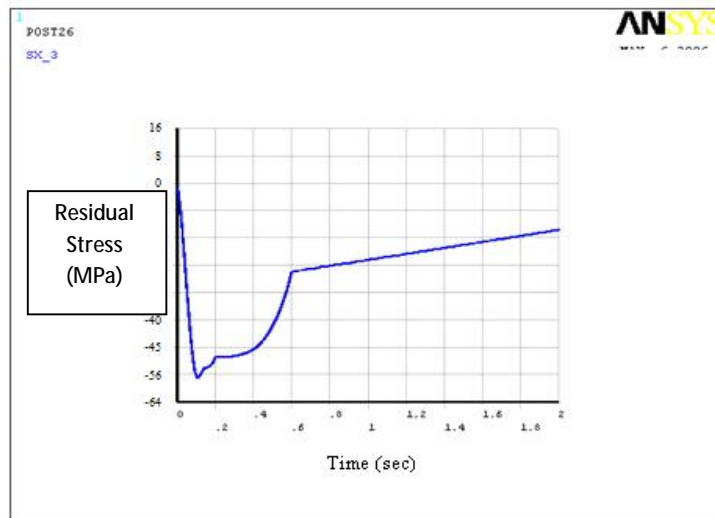


Figure (12): Longitudinal Stress History Away From Spot Center.

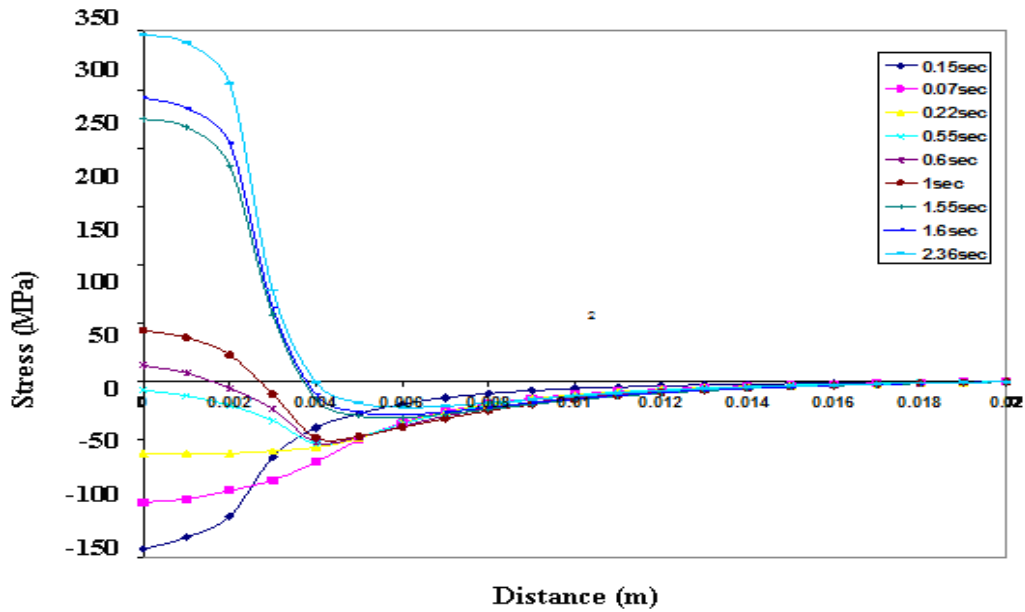


Figure (13): Stress Distribution from Center Spot to the Left at Different Times.

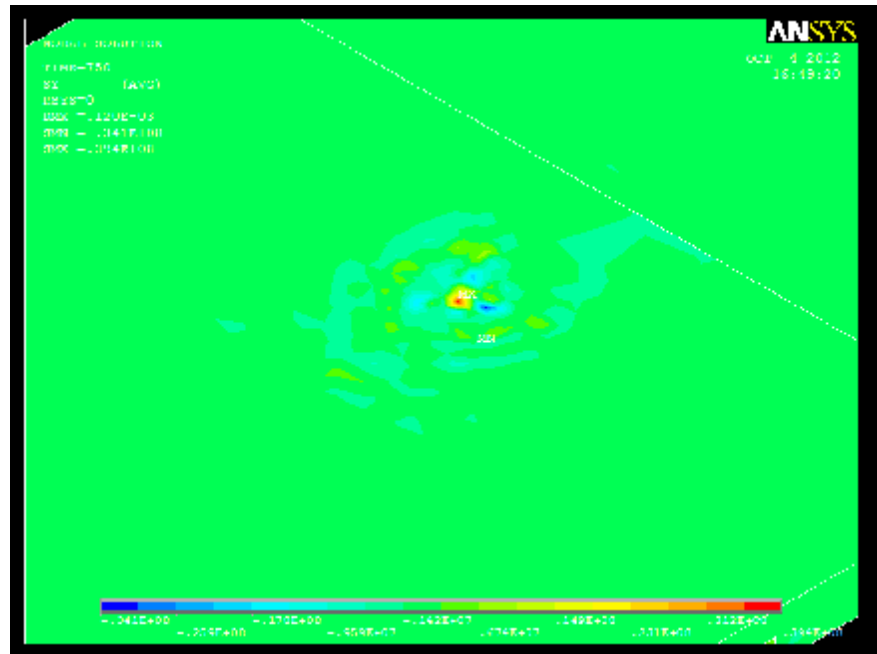


Figure (14): Residual Stress Distribution in the Y-Direction for second spot, Group (D).

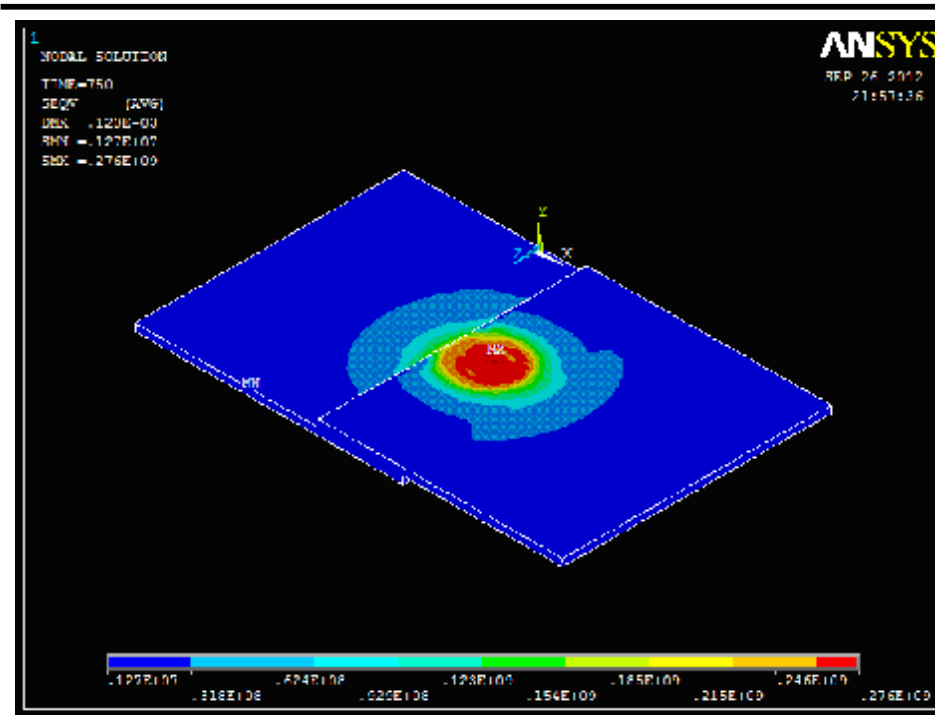


Figure (15): Von Mises Residual Stress Distribution for second spot, Group (D).

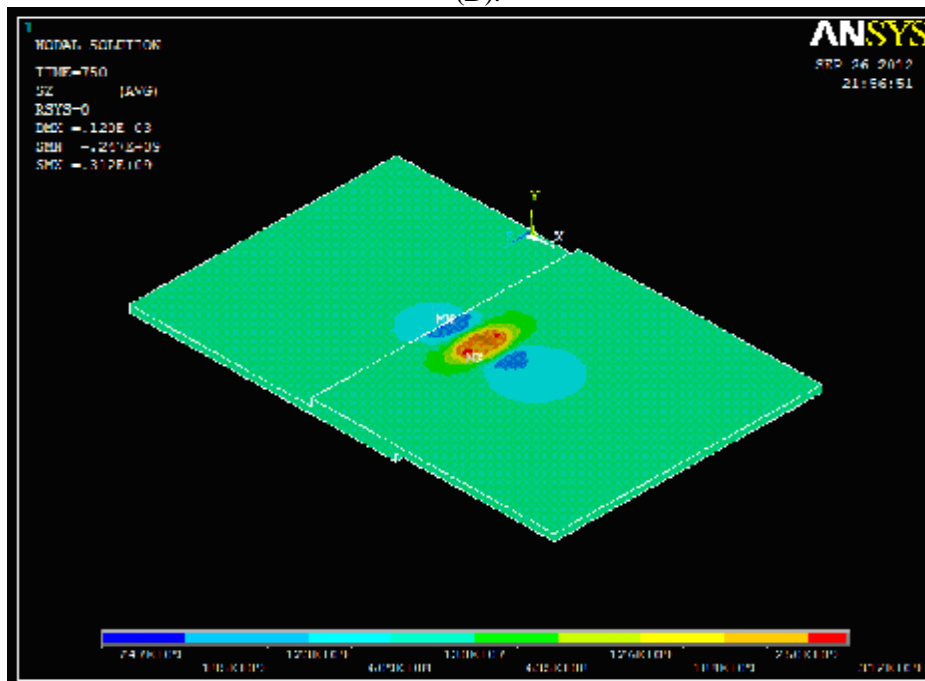


Figure (16): Residual Stress Distribution in the X-Z Direction for second spot, Group (D).

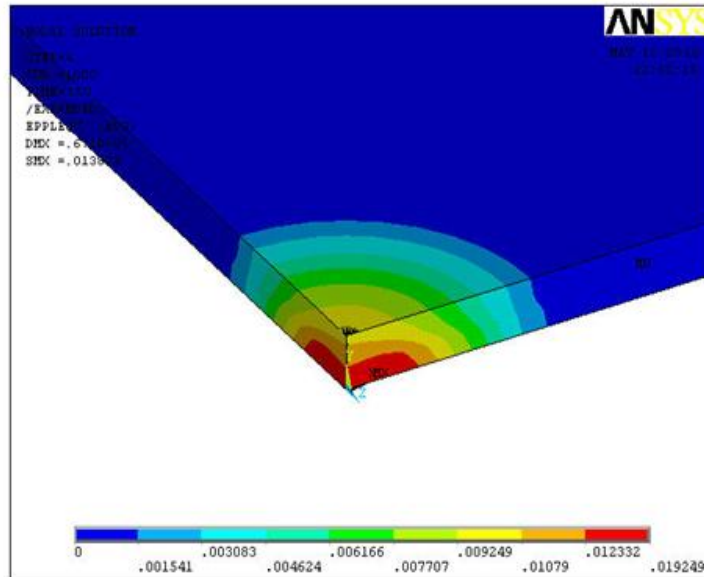


Figure (17): Von Mises Plastic Strain Distribution at final weld shape.

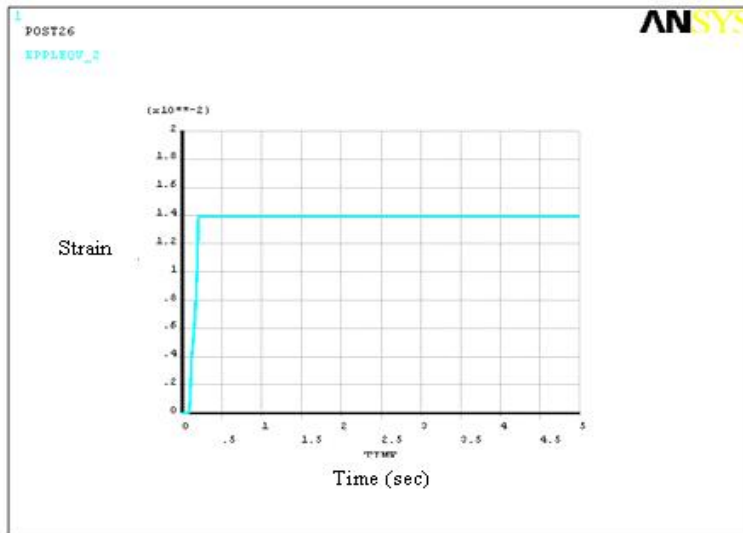


Figure (18): Von Mises Plastic Strain History at Nugget Center.

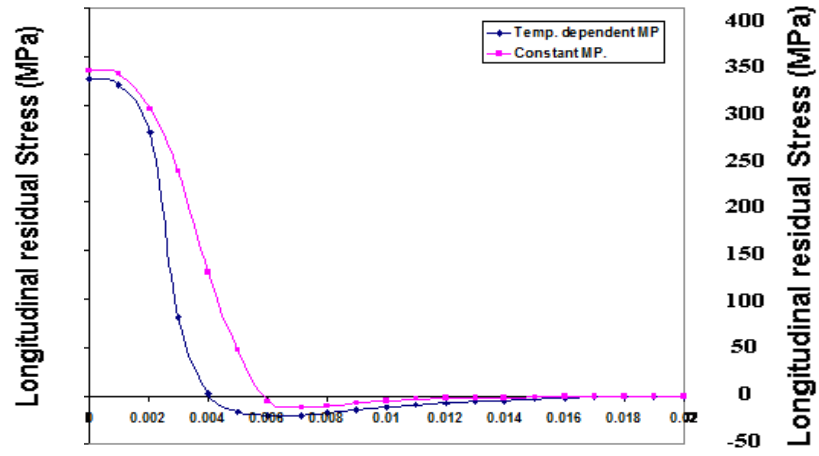


Figure (19): Effect of Material Properties on Longitudinal Residual.